gases

MDPI

Article

Electrostatic Shock Structures in a Magnetized Plasma Having Non-Thermal Particles

Sharmin Jahan [1,*], Subrata Banik [2], Nure Alam Chowdhury [3], Abdul Mannan [1] and A A Mamun [1]

[1] Department of Physics, Jahangirnagar University, Dhaka 1342, Bangladesh; abdulmannan@juniv.edu (A.M.); mamun_phys@juniv.edu (A.A.M.)
[2] Atomic Energy Centre, Health Physics Division, Dhaka 1000, Bangladesh; bsubrata.37@gmail.com
[3] Atomic Energy Centre, Plasma Physics Division, Dhaka 1000, Bangladesh; nurealam1743phy@gmail.com
* Correspondence: jahan88phy@gmail.com

Abstract: A rigorous theoretical investigation has been made on the nonlinear propagation of dust-ion-acoustic shock waves in a multi-component magnetized pair-ion plasma (PIP) having inertial warm positive and negative ions, inertialess non-thermal electrons and positrons, and static negatively charged massive dust grains. The Burgers' equation is derived by employing the reductive perturbation method. The plasma model supports both positive and negative shock structures in the presence of static negatively charged massive dust grains. It is found that the steepness of both positive and negative shock profiles declines with the increase of ion kinematic viscosity without affecting the height, and the increment of negative (positive) ion mass in the PIP system declines (enhances) the amplitude of the shock profile. It is also observed that the increase in oblique angle raises the height of the positive shock profile, and the height of the positive shock wave increases with the number density of positron. The applications of the findings from the present investigation are briefly discussed.

Keywords: pair-ion plasma; Burgers' equation; shock waves; magnetized plasma

Citation: Jahan, S.; Banik, S.; Chowdhury, N.A.; Mannan, A.; Mamun, A.A. Electrostatic Shock Structures in a Magnetized Plasma Having Non-Thermal Particles. *Gases* **2022**, *2*, 22–32. https://doi.org/10.3390/gases2020002

Academic Editor: Ben J. Anthony

Received: 17 January 2022
Accepted: 22 March 2022
Published: 25 March 2022

1. Introduction

Positive ions are produced by the electron impact ionization while negative ions are produced due to the attachment of electron with an atom [1], and the existence of both positive and negative ions or pair-ion (PI) can be observed in space plasmas, viz., cometary comae [2], upper regions of Titan's atmosphere [3–5], plasmas in the D- and F-regions of Earth's ionosphere [4–6]), and also laboratory plasmas, viz., (K^+, SF_6^-) plasma [7,8], (Ar^+, F^-) plasma [9], plasma processing reactors [10], plasma etching [11], combustion products [11], (Xe^+, F^-) plasma [12], neutral beam sources [13], (Ar^+, SF_6^-) plasma [14–16], (Ar^+, O_2^-) plasma, Fullerene (C_{60}^+, C_{60}^-) plasma [17,18], etc. The dynamics of the plasma system and associated nonlinear electrostatic structures have been rigorously changed by the presence of massive dust grains in the PI plasma (PIP) [19–22]. Yasmin et al. [23] studied the nonlinear propagation of dust-ion-acoustic (DIA) waves (DIAWs) in a multi-component plasma and found that the shock profile associated with DIAWs is significantly modified by the existence of dust grains. A number of authors also examined the effects of the positron to the formation of solitary profile associated with electrostatic waves [24,25]. Rahman et al. [24] studied the electrostatic solitary waves in electron-positron-ion plasma, and observed that the amplitude of the solitary profile increases with increasing the number density of positron. Abdelsalam [25] investigated ion-acoustic (IA) solitary waves in a dense plasma, and demonstrated that the presence of the positron can cause an increase in the amplitude of the solitary profile.

Cairns et al. [26] first demonstrated the non-thermal distribution to investigate the effect of energetic particles on the formation of IA shock profile, and introduced the parameter α in the non-thermal distribution for measuring the amount of deviation of

non-thermal plasma species from Maxellian–Boltzmann distribution. The non-thermal plasma species are regularly seen in the cometary comae [2], Earth's ionosphere [4], the upper region of the Titans [3], etc. Haider et al. [27] investigated the IA solitary waves in the presence of non-thermal particles, and observed that the width of the solitary profile decreases with increasing of ions' non-thermality. Pakzad and Javidan [28] studied the dust-acoustic (DA) solitary and shock waves in a dusty plasma having non-thermal ions, and reported that the amplitude of the wave increases with the decrease of the non-thermality of ions. Ghai et al. [29] studied the DA solitary waves in the presence of non-thermal ions, and found that the height of the solitary wave decreases with the increase of α.

Landau damping and the kinematic viscosity among the plasma species are the primary reasons for the formation of shock profile associated with electrostatic waves [30–32]. The existence of the external magnetic field is considered to be responsible for changing the configuration of the shock profile [33]. Sabetkar and Dorranian [30] examined the effects of external magnetic field on the formation of the DA solitary waves in the presence of non-thermal plasma species, and found that the amplitude of solitary wave increases with the increase in the value of oblique angle. Shahmansouri and Mamun [31] analyzed the DA shock waves in a magnetized non-thermal dusty plasma and demonstrated that the amplitude of shock wave increases with increasing the oblique angle. Malik et al. [32] studied the small-amplitude DA wave in magnetized plasma, and reported that the height of the shock wave enhances with oblique angle. Bedi et al. [34] studied DA solitary waves in a four-component magnetized dusty plasma, and highlighted that both compressive and rarefactive solitons can exist in the presence of an external magnetic field. To the best knowledge of the authors, no attempt has been made to study the DIA shock waves (DIASHWs) in a magnetized PIP by considering kinematic viscosity of both inertial warm positive and negative ion species, and inertialess non-thermal electrons and positrons in the presence of static negatively charged dust grains. The aim of our present investigation is, therefore, to derive Burgers' equation and investigate DIASHWs in a magnetized PIP, and to observe the effects of various plasma parameters (e.g., mass, charge, temperature, kinematic viscosity, obliqueness, etc.) on the configuration of DIASHWs.

The layout of the paper is as follows: The basic equations are displayed in Section 2. The well known Burgers' equation is derived in Section 3. Numerical analysis and discussion are presented in Section 4. A brief conclusion is given in Section 5.

2. Governing Equations

We consider a multi-component PIP having inertial positively charged warm ions (mass m_1; charge eZ_1; temperature T_1; number density $\tilde{n_1}$), negatively charged warm ions (mass m_2; charge $-eZ_2$; temperature T_2; number density $\tilde{n_2}$), inertialess electrons featuring non-thermal distribution (mass m_e; charge $-e$; temperature T_e; number density $\tilde{n_e}$), inertialess positrons obeying non-thermal distribution (mass m_p; charge e; temperature T_p; number density $\tilde{n_p}$), and static negatively charged massive dust grains (charge $-eZ_d$; number density n_d); where Z_1 (Z_2) is the charge state of the positive (negative) ion, and Z_d is the charge state of the negative dust grains, and e is the magnitude of the charge of an electron. An external magnetic field $\mathbf{B}_0$ is considered in the system directed along the z-axis defining $\mathbf{B}_0 = B_0\hat{z}$, where B_0 and $\hat{z}$ denote the strength of the external magnetic field and unit vector directed along the z-axis, respectively. The dynamics of the PIP system is governed by the following set of equations [35–39]:

$$\frac{\partial \tilde{n}_1}{\partial \tilde{t}} + \tilde{\nabla} \cdot (\tilde{n}_1 \tilde{u}_1) = 0, \tag{1}$$

$$\frac{\partial \tilde{u}_1}{\partial \tilde{t}} + (\tilde{u}_1 \cdot \tilde{\nabla})\tilde{u}_1 = -\frac{Z_1 e}{m_1}\tilde{\nabla}\tilde{\psi} + \frac{Z_1 e B_0}{m_1}(\tilde{u}_1 \times \hat{z}) - \frac{1}{m_1 \tilde{n}_1}\tilde{\nabla} P_1 + \tilde{\eta}_1 \tilde{\nabla}^2 \tilde{u}_1, \tag{2}$$

$$\frac{\partial \tilde{n}_2}{\partial \tilde{t}} + \tilde{\nabla} \cdot (\tilde{n}_2 \tilde{u}_2) = 0, \tag{3}$$

$$\frac{\partial \tilde{u}_2}{\partial \tilde{t}} + (\tilde{u}_2 \cdot \tilde{\nabla})\tilde{u}_2 = \frac{Z_2 e}{m_2}\tilde{\nabla}\tilde{\psi} - \frac{Z_2 e B_0}{m_2}(\tilde{u}_2 \times \hat{z}) - \frac{1}{m_2 \tilde{n}_2}\tilde{\nabla} P_2 + \tilde{\eta}_2 \tilde{\nabla}^2 \tilde{u}_2, \tag{4}$$

$$\tilde{\nabla}^2 \tilde{\psi} = 4\pi e[\tilde{n}_e + Z_d \tilde{n}_d + Z_2 \tilde{n}_2 - Z_1 \tilde{n}_1 - \tilde{n}_p], \tag{5}$$

where $\tilde{u}_1$ ($\tilde{u}_2$) is the positive (negative) ion fluid velocity; $\tilde{\eta}_1 = \mu_1/m_1 n_1$ ($\tilde{\eta}_2 = \mu_2/m_2 n_2$) is the kinematic viscosity of the positive (negative) ion; P_1 (P_2) is the pressure of positive (negative) ion, and $\tilde{\psi}$ represents the electrostatic wave potential. Now, we are introducing normalized variables, namely, $n_1 \to \tilde{n}_1/n_{10}$, $n_2 \to \tilde{n}_2/n_{20}$, $n_e \to \tilde{n}_e/n_{e0}$, $n_p \to \tilde{n}_p/n_{p0}$, $n_d \to \tilde{n}_d/n_{d0}$, $u_1 \to \tilde{u}_1/C_2$, $u_2 \to \tilde{u}_2/C_2$ (where $C_2 = (Z_2 k_B T_e/m_2)^{1/2}$, k_B being the Boltzmann constant); $\psi \to \tilde{\psi} e/k_B T_e$; $t = \tilde{t}/\omega_{P_2}^{-1}$ [where $\omega_{P_2}^{-1} = (m_2/4\pi e^2 Z_2^2 n_{20})^{1/2}$]; $\tilde{\nabla} = \nabla/\lambda_D$ (where $\lambda_D = (k_B T_e/4\pi e^2 Z_2 n_{20})^{1/2}$). The pressure term of the positive ion can be recognized as $P_1 = P_{10}(\tilde{n}_1/n_{10})^{\gamma}$ with $P_{10} = n_{10} k_B T_1$ being the equilibrium pressure of the positive ion, and the pressure term of the negative ion can be recognized as $P_2 = P_{20}(\tilde{n}_2/n_{20})^{\gamma}$ with $P_{20} = n_{20} k_B T_2$ being the equilibrium pressure of the negative ion, and $\gamma = (N+2)/N$ (where N is the degree of freedom, and for a three-dimensional case, $N = 3$, then $\gamma = 5/3$). For simplicity, we consider ($\tilde{\eta}_1 \approx \tilde{\eta}_2 = \eta$), and η is normalized by $\omega_{P_2}\lambda_D^2$. The quasi-neutrality condition at equilibrium for our plasma model can be written as $Z_1 n_{10} + n_{p0} \approx Z_2 n_{20} + Z_d n_{d0} + n_{e0}$. Equations (1)–(5) can be expressed in the normalized form as [40]:

$$\frac{\partial n_1}{\partial t} + \nabla \cdot (n_1 u_1) = 0, \tag{6}$$

$$\frac{\partial u_1}{\partial t} + (u_1 \cdot \nabla)u_1 = -\alpha_1 \nabla \psi + \alpha_1 \Omega_c (u_1 \times \hat{z}) - \alpha_2 \nabla n_1^{\gamma - 1} + \eta \nabla^2 u_1, \tag{7}$$

$$\frac{\partial n_2}{\partial t} + \nabla \cdot (n_2 u_2) = 0, \tag{8}$$

$$\frac{\partial u_2}{\partial t} + (u_2 \cdot \nabla)u_2 = \nabla \psi - \Omega_c (u_2 \times \hat{z}) - \alpha_3 \nabla n_2^{\gamma - 1} + \eta \nabla^2 u_2, \tag{9}$$

$$\nabla^2 \psi = \lambda_e n_e - \lambda_p n_p + \lambda_d n_d - (1 + \lambda_e + \lambda_d - \lambda_p) n_1 + n_2. \tag{10}$$

Other plasma parameters can be recognized as $\alpha_1 = Z_1 m_2/Z_2 m_1$, $\alpha_2 = 5T_1 m_2/2Z_2 T_e m_1$, $\alpha_3 = 5T_2/2Z_2 T_e$, $\lambda_e = n_{e0}/Z_2 n_{20}$, $\lambda_d = Z_d n_{d0}/Z_2 n_{20}$, $\lambda_p = n_{p0}/Z_2 n_{20}$, and $\Omega_c = \omega_c/\omega_{P_2}$ (where $\omega_c = Z_2 e B_0/m_2$). Now, the expression for the number density of electrons [26,41–43] and positrons [26,44] following non-thermal distribution can be, respectively, written as

$$n_e = (1 - \beta\psi + \beta\psi^2)\exp(\psi), \tag{11}$$

$$n_p = (1 + \beta\alpha_4\psi + \beta\alpha_4^2\psi^2)\exp(-\alpha_4\psi), \tag{12}$$

where $\beta = 4\alpha/(1+3\alpha)$ (α represents the number of non-thermal populations in our considered model) and $\alpha_4 = T_e/T_p$. Now, by substituting Equations (11) and (12) into Equation (10), and expanding up to the third order in ψ, we can write

$$\nabla^2 \psi = \lambda_e - \lambda_p + n_d \lambda_d + n_2 - \Lambda n_1 + \sigma_1 \psi + \sigma_2 \psi^2 + \cdots, \tag{13}$$

where $\Lambda = 1 + \lambda_e + \lambda_d - \lambda_p$, $\sigma_1 = \lambda_e(1-\beta) - \lambda_p \alpha_4 (\beta - 1)$, and $\sigma_2 = \lambda_e/2 - \lambda_p \alpha_4^2/2$. We note that the terms containing σ_1 and σ_2 are the contribution of non-thermal distributed electrons and positrons.

3. Derivation of Burgers' Equation

To derive Burgers' equation [45–47] for the DIASHWs propagating in a PIP, we first introduce the stretched co-ordinates [48,49] as

$$\xi = \epsilon(l_x x + l_y y + l_z z - V_p t), \tag{14}$$

$$\tau = \epsilon^2 t, \tag{15}$$

where V_p is the phase speed and ϵ is a smallness parameter denoting the weakness of the dissipation ($0 < \epsilon < 1$). It is noted that l_x, l_y, and l_z (i.e., $l_x^2 + l_y^2 + l_z^2 = 1$) are the directional cosines of the wave vector of k along x, y, and z-axes, respectively. Then, the dependent variables can be expressed in power series of ϵ as [49]

$$n_1 = 1 + \epsilon n_1^{(1)} + \epsilon^2 n_1^{(2)} + \epsilon^3 n_1^{(3)} + \cdots, \tag{16}$$

$$n_2 = 1 + \epsilon n_2^{(1)} + \epsilon^2 n_2^{(2)} + \epsilon^3 n_2^{(3)} + \cdots, \tag{17}$$

$$u_{1x,y} = \epsilon^2 u_{1x,y}^{(1)} + \epsilon^3 u_{1x,y}^{(2)} + \cdots, \tag{18}$$

$$u_{2x,y} = \epsilon^2 u_{2x,y}^{(1)} + \epsilon^3 u_{2x,y}^{(2)} + \cdots, \tag{19}$$

$$u_{1z} = \epsilon u_{1z}^{(1)} + \epsilon^2 u_{1z}^{(2)} + \cdots, \tag{20}$$

$$u_{2z} = \epsilon u_{2z}^{(1)} + \epsilon^2 u_{2z}^{(2)} + \cdots, \tag{21}$$

$$\psi = \epsilon \psi^{(1)} + \epsilon^2 \psi^{(2)} + \cdots. \tag{22}$$

Now, by substituting Equations (14)–(22) into Equations (6)–(9) and (13), and collecting the terms containing ϵ, the first-order equations become

$$n_1^{(1)} = \frac{3\alpha_1 l_z^2}{3V_p^2 - 2\alpha_2 l_z^2}\psi^{(1)}, \tag{23}$$

$$u_{1z}^{(1)} = \frac{3V_p \alpha_1 l_z}{3V_p^2 - 2\alpha_2 l_z^2}\psi^{(1)}, \tag{24}$$

$$n_2^{(1)} = -\frac{3l_z^2}{3V_p^2 - 2\alpha_3 l_z^2}\psi^{(1)}, \tag{25}$$

$$u_{2z}^{(1)} = -\frac{3V_p l_z}{3V_p^2 - 2\alpha_3 l_z^2}\psi^{(1)}. \tag{26}$$

Now, the phase speed of DIASHWs can be read as

$$V_p \equiv V_{p+} = l_z \sqrt{\frac{-a_1 + \sqrt{a_1^2 - 36\sigma_1 a_2}}{18\sigma_1}}, \tag{27}$$

$$V_p \equiv V_{p-} = l_z \sqrt{\frac{-a_1 - \sqrt{a_1^2 - 36\sigma_1 a_2}}{18\sigma_1}}, \tag{28}$$

where $a_1 = -(6\sigma_1\alpha_2 + 6\sigma_1\alpha_3 + 9 + \Lambda n_1)$ and $a_2 = 4\sigma_1\alpha_2\alpha_3 + 6\alpha_2 + 6\alpha_1\alpha_3\Lambda$. The x and y-components of the first-order momentum equations can be written as

$$u_{1x}^{(1)} = -\frac{3l_y V_p^2}{\Omega_c(3V_p^2 - 2\alpha_2 l_z^2)} \frac{\partial \psi^{(1)}}{\partial \xi}, \tag{29}$$

$$u_{1y}^{(1)} = \frac{3l_x V_p^2}{\Omega_c(3V_p^2 - 2\alpha_2 l_z^2)} \frac{\partial \psi^{(1)}}{\partial \xi}, \tag{30}$$

$$u_{2x}^{(1)} = -\frac{3l_y V_p^2}{\Omega_c(3V_p^2 - 2\alpha_3 l_z^2)} \frac{\partial \psi^{(1)}}{\partial \xi}, \tag{31}$$

$$u_{2y}^{(1)} = \frac{3l_x V_p^2}{\Omega_c(3V_p^2 - 2\alpha_3 l_z^2)} \frac{\partial \psi^{(1)}}{\partial \xi}. \tag{32}$$

Now, by following the next higher-order terms, the equation of continuity, momentum equation, and Poisson's equation can be written as

$$\frac{\partial n_1^{(1)}}{\partial \tau} - V_p \frac{\partial n_1^{(2)}}{\partial \xi} + l_x \frac{\partial u_{1x}^{(1)}}{\partial \xi} + l_y \frac{\partial u_{1y}^{(1)}}{\partial \xi} + l_z \frac{\partial u_{1z}^{(2)}}{\partial \xi} + l_z \frac{\partial}{\partial \xi}\left(n_1^{(1)} u_{+z}^{(1)}\right) = 0, \tag{33}$$

$$\frac{\partial u_{1z}^{(1)}}{\partial \tau} - V_p \frac{\partial u_{1z}^{(2)}}{\partial \xi} + l_z u_{1z}^{(1)} \frac{\partial u_{1z}^{(1)}}{\partial \xi} + \alpha_1 l_z \frac{\partial \psi^{(2)}}{\partial \xi} + \alpha_2 l_z \frac{\partial}{\partial \xi}\left[\frac{2}{3} n_1^{(2)} - \frac{1}{9}(n_1^{(1)})^2\right] - \eta \frac{\partial^2 u_{1z}^{(1)}}{\partial \xi^2} = 0, \tag{34}$$

$$\frac{\partial n_2^{(1)}}{\partial \tau} - V_p \frac{\partial n_2^{(2)}}{\partial \xi} + l_x \frac{\partial u_{2x}^{(1)}}{\partial \xi} + l_y \frac{\partial u_{2y}^{(1)}}{\partial \xi} + l_z \frac{\partial u_{2z}^{(2)}}{\partial \xi} + l_z \frac{\partial}{\partial \xi}\left(n_2^{(1)} u_{2z}^{(1)}\right) = 0, \tag{35}$$

$$\frac{\partial u_{2z}^{(1)}}{\partial \tau} - V_p \frac{\partial u_{2z}^{(2)}}{\partial \xi} + l_z u_{2z}^{(1)} \frac{\partial u_{2z}^{(1)}}{\partial \xi} - l_z \frac{\partial \psi^{(2)}}{\partial \xi} + \alpha_3 l_z \frac{\partial}{\partial \xi}\left[\frac{2}{3} n_2^{(2)} - \frac{1}{9}(n_2^{(1)})^2\right] - \eta \frac{\partial^2 u_{2z}^{(1)}}{\partial \xi^2} = 0, \tag{36}$$

$$\sigma_1 \psi^{(2)} + \sigma_2 [\psi^{(1)}]^2 + n_2^{(2)} - \Lambda n_1^{(2)} = 0. \tag{37}$$

Finally, the next higher-order terms of Equations (6)–(9) and (13), with the help of Equations (23)–(37), can provide Burgers' equation as

$$\frac{\partial \Psi}{\partial \tau} + A\Psi \frac{\partial \Psi}{\partial \xi} = C \frac{\partial^2 \Psi}{\partial \xi^2}, \tag{38}$$

where $\Psi = \psi^{(1)}$ is used for simplicity. In Equation (38), the nonlinear coefficient (A) and dissipative coefficient (C) are given by the following expression:

$$A = \frac{(M_1 S_1^3 - M_2 S_2^3 - 2\sigma_2 S_1^3 S_2^3)}{M_3 S_1 S_2}, \text{ and } C = \frac{\eta}{2}, \tag{39}$$

where $M_1 = \Lambda(81\alpha_1^2 V_p^2 l_z^4 - 6\alpha_2 \alpha_1^2 l_z^6)$, $M_2 = 81 V_p^2 l_z^4 - 6\alpha_3 l_z^6$, and $M_3 = 18 V_p l_z^2 (1 + \alpha_1 \Lambda)$. It is well established that the ion fluids are viscous, and in realistic situations, ion fluids which occur in both space [50] and laboratory [50,51] plasmas, where the effect of viscous force cannot be neglected. It is important to note here that Burger's equation, defined by Equation (38), is derived for our multi-ion dusty plasma system, when the effect of dispersion is negligible compared to that of dissipation.

Now, we look forward to the stationary shock wave solution of this Burgers' equation by taking $\zeta = \xi - U_0 \tau'$ and $\tau = \tau'$, where U_0 is the speed of the shock waves in the reference frame. These allow us to represent the stationary shock wave solution as [49,52,53]

$$\Psi = \Psi_m \left[1 - \tanh\left(\frac{\zeta}{\Delta}\right)\right], \tag{40}$$

where Ψ_m is the amplitude and Δ is the width. The expression of the amplitude and width can be given by the following equations:

$$\Psi_m = \frac{U_0}{A}, \quad \text{and} \quad \Delta = \frac{2C}{U_0}. \tag{41}$$

4. Numerical Analysis and Discussion

Now, we would like to observe the basic properties of DIASHWs in a magnetized PIP having inertial pair-ions, inertialess non-thermal distributed electrons and positrons, and static negatively charged massive dust grains by changing the various plasma parameters, viz., ion kinematic viscosity, oblique angle, non-thermality of electrons and positrons, mass, charge, and number density of the plasma species. Note that the viscous force acting in positive and negative ion fluid of the plasma model under consideration is the source of dissipation, and is responsible for the formation of shock structures [50]. It can be seen from the literature that the PIP system can support these conditions: $m_2 > m_1$ (i.e., $H^+ - O_2^-$ [8,10,13–16], $Ar^+ - SF_6^-$ [14–16,54], and $Xe^+ - SF_6^-$ [14–16,54]), $m_2 = m_1$ (i.e., $H^+ - H^-$ [8,10,13–16] and $C_{60}^+ - C_{60}^-$ [17,18,55]), and $m_2 < m_1$ (i.e., $Ar^+ - F^-$ [10,13]). Equation (41) shows that under consideration of $U_0 > 0$ and $C > 0$, no shock wave will exist if $A = 0$ as the amplitude of the wave becomes infinite, which clearly violates the reductive perturbation method [56–59]. Thus, A can be positive (i.e., $A > 0$) or negative (i.e., $A < 0$), according to the value of other plasma parameters. The left panel of Figure 1 illustrates the variation of A with α_4, and it is obvious from this figure that A can be negative, zero, and positive according to the values of α_4 when other plasma parameters are $\alpha_1 = 1.5$, $\alpha_2 = 0.05$, $\alpha_3 = 0.03$, $\lambda_p = 1.5$, $\lambda_e = 1.7$, $\lambda_d = 0.05$, $\delta = 30^\circ$, and $\alpha = 0.5$. The point at which A becomes zero for the value of α_4 is known as the critical value of α_4 (i.e., α_{4c}). In our present analysis, the critical value of α_4 is $\alpha_{4c} \equiv 01$. Thus, the negative (positive) shock profile can exist for the value of $\alpha_4 < \alpha_{4c}$ ($\alpha_4 > \alpha_{4c}$). The right panel of Figure 1 describes the effects of the external magnetic field on the formation of the positive shock profile. The increase in oblique angle raises the height of the positive shock profile, and this result is analogous to the result of Ref. [31].

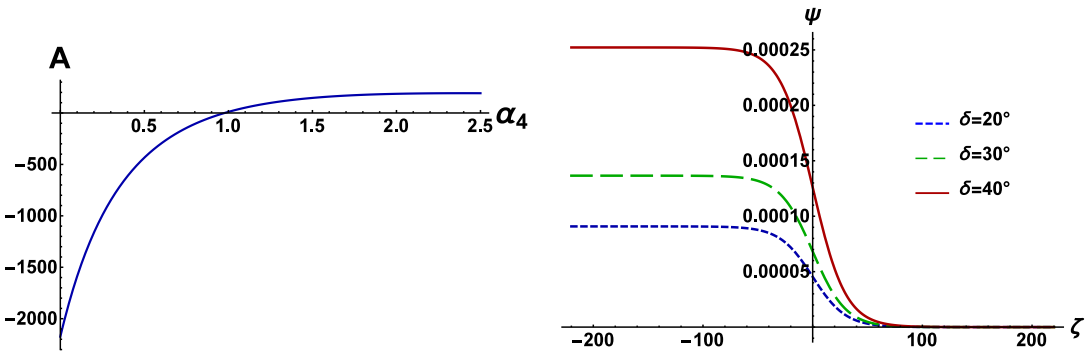

Figure 1. The variation of nonlinear coefficient A with α_4 (**left panel**) and Ψ with ζ for different values of δ (**right panel**) along with $\alpha_1 = 1.5$, $\alpha_2 = 0.05$, $\alpha_3 = 0.03$, $\lambda_p = 1.5$, $\lambda_e = 1.7$, $\lambda_d = 0.05$, $\alpha = 0.5$, and $V_p \equiv V_{p+}$.

The left and right panels of Figure 2 represent the variation of the positive and negative shock profiles with ion kinematic viscosity (via η), respectively, when other plasma parameters remain constant. It is really interesting that the steepness of both positive and negative shock profiles declines with the increase of η without affecting the height.

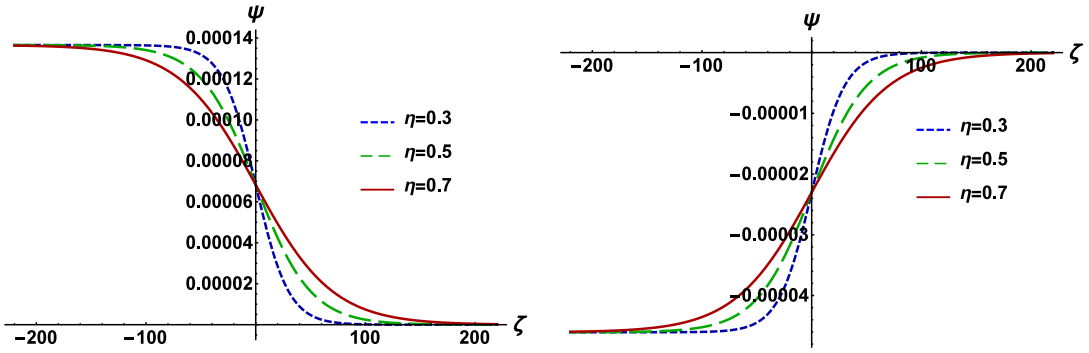

Figure 2. The variation of Ψ with ζ for different values of η under consideration of $\alpha_4 > \alpha_{4c}$ (**left panel**) and $\alpha_4 < \alpha_{4c}$ (**right panel**) along with $\alpha_1 = 1.5$, $\alpha_2 = 0.05$, $\alpha_3 = 0.03$, $\lambda_p = 1.5$, $\lambda_e = 1.7$, $\lambda_d = 0.05$, $\delta = 30^\circ$, $\alpha = 0.5$, $U_0 = 0.01$, and $V_p \equiv V_{p+}$.

The height of the positive shock profile is very sensitive to the change of non-thermality of the electrons and positrons, which can be seen in the left panel of Figure 3. There is a decrease in the amplitude of positive shock profile when electrons and positrons deviate from thermodynamic equilibrium, and this result is compatible with the result of Ref. [60]. The variation of the DIASHWs with negative ion charge state, negative ion, and positron number densities (via λ_p) can be observed in the right panel of Figure 3. It is clear from the right panel of Figure 3 that as we increase the positron (negative ion) number density, the height of the positive shock wave increases (decreases) when the charge of the negative ion remains constant, or the the height of the positive shock wave decreases with the charge of the negative ion for a fixed value of the number density of positron and negative ion.

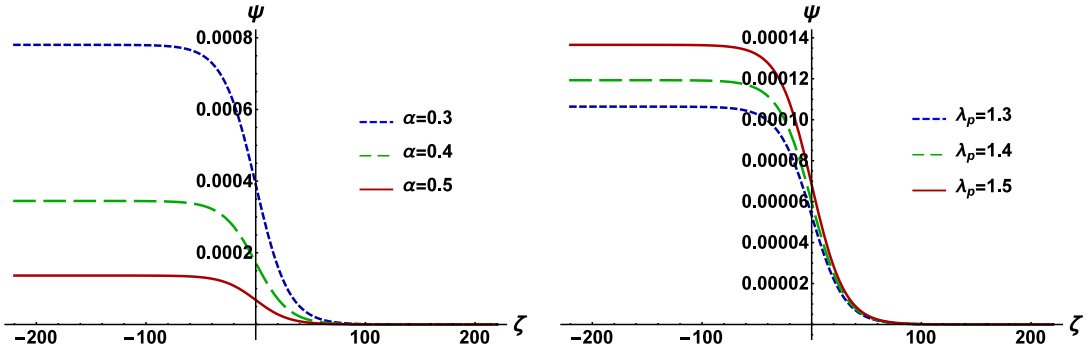

Figure 3. The variation of Ψ with ζ for different values of α (**left panel**) and λ_p (**right panel**) under consideration of $\alpha_4 > \alpha_{4c}$ along with $\alpha_1 = 1.5$, $\alpha_2 = 0.05$, $\alpha_3 = 0.03$, $\alpha_4 = 1.5$, $\lambda_e = 1.7$, $\lambda_d = 0.05$, $\delta = 30^\circ$, $\eta = 0.3$, $U_0 = 0.01$, and $V_p \equiv V_{p+}$.

The charge and mass of the positive and negative ions are vigorously responsible for changing the height of the positive shock profile. Figure 4 describes the nature of DIASHWs with the variation values of α_1, i.e., $\alpha_1 > 1$ (left panel) and α_1, i.e., $\alpha_1 < 1$ (right panel), respectively, under consideration of $\alpha_4 > \alpha_{4c}$. it is obvious from this figure that (a) due to the $\alpha_4 > \alpha_{4c}$, we have observed positive shock potential of DIASWs; (b) the height of the positive shock profile increases (decreases) with rising value of positive (negative) ion mass for a fixed value of the their charge state, but as we increase the charge state of the positive (negative) ion, then the amplitude of the positive shock profile diminishes (enhances) when their masses are constant; (c) the height of the amplitude of the shock profile is taller (shorter) under the assumption of $m_2 < m_1$ ($m_2 > m_1$). Thus, the dynamics of positive shock profile of DIASWs in PIP system rigorously change with these conditions $m_2 < m_1$ (i.e., $\alpha_1 < 1$) and $m_2 > m_1$ (i.e., $\alpha_1 > 1$).

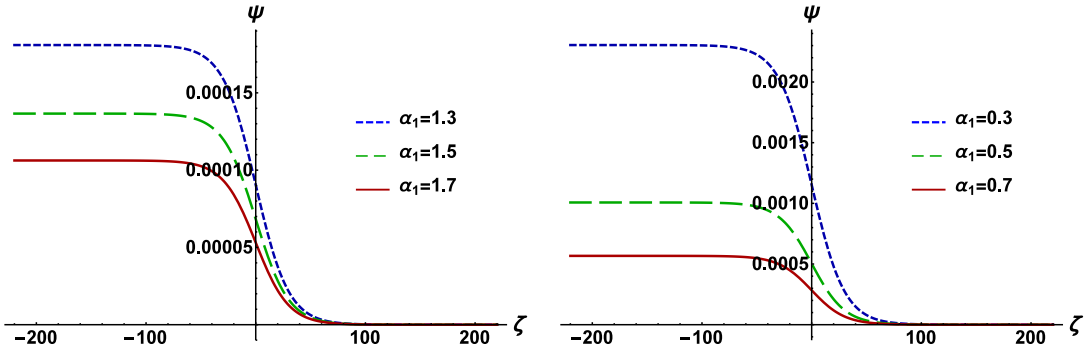

Figure 4. The variation of Ψ with ζ for different values of α_1, i.e., $\alpha_1 > 1$ (**left panel**) and α_1, i.e., $\alpha_1 < 1$ (**right panel**) under consideration of $\alpha_4 > \alpha_{4c}$ along with $\alpha_3 = 0.03$, $\alpha_4 = 1.5$, $\lambda_e = 1.7$, $\lambda_p = 1.5$, $\lambda_d = 0.05$, $\delta = 30^\circ$, $\eta = 0.3$, $\alpha = 0.5$, $U_0 = 0.01$, and $V_p \equiv V_{p+}$.

We can also observe the effects of mass and charge of positive and negative ions in the formation of the negative shock profile from Figure 5 under consideration of $\alpha_4 < \alpha_{4c}$. The left panel represents the variation of potential with ξ under consideration of $m_2 > m_1$, i.e., $\alpha > 1$, while the right panel represents the variation of potential with ξ under consideration of $m_2 < m_1$, i.e., $\alpha < 1$. It can be seen from this figure that the magnitude of the amplitude decreases (increases) with the mass of negative (positive) ion when their charge remains constant. Physically, the order of the variation of the potential, as well as the dynamics of the plasma medium, is invariant under the conditions $m_2 > m_1$ or $m_2 < m_1$.

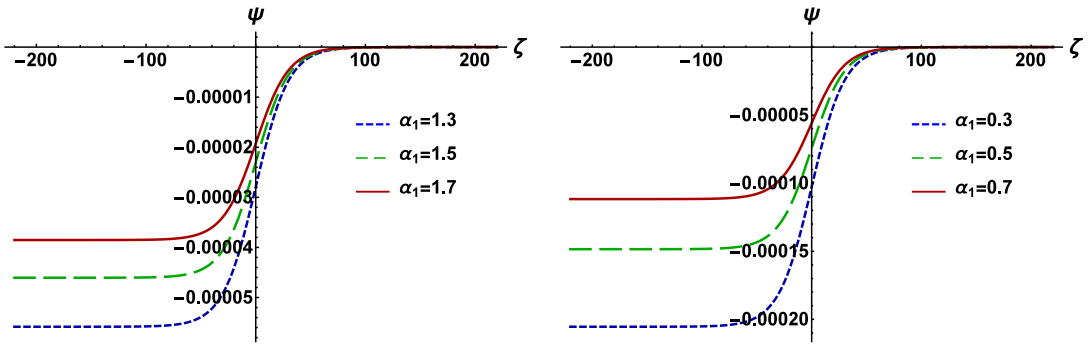

Figure 5. The variation of Ψ with ζ for different values of α_1, i.e., $\alpha_1 > 1$ (**left panel**) and α_1, i.e., $\alpha_1 < 1$ (**right panel**) under consideration of $\alpha_4 < \alpha_{4c}$ along with $\alpha_3 = 0.03$, $\alpha_4 = 1.5$, $\lambda_e = 1.7$, $\lambda_p = 1.5$, $\lambda_d = 0.05$, $\delta = 30^\circ$, $\eta = 0.3$, $\alpha = 0.5$, $U_0 = 0.01$, and $V_p \equiv V_{p+}$.

5. Conclusions

In our present investigation, we considered a multi-component magnetized PIP having static dust grains, non-thermal electrons, and positrons. Burgers' equation was derived by employing the reductive perturbation method for studying DIASHWs. The results that we have found from this investigation can be summarized as follows:

- The negative (positive) shock profile can exist for the value of $\alpha_4 < \alpha_{4c}$ ($\alpha_4 > \alpha_{4c}$).
- The steepness of both positive and negative shock profiles declines with the increase of η without affecting the height.
- The increase in oblique angle raises the height of the positive shock profile.
- The height of the positive shock wave increases with the number density of positron.
- The amplitude of the positive shock profile increases (decreases) with increasing the value of positive (negative) ion mass.

The results are applicable in understanding the criteria for the formation of DIASHWs in astrophysical plasmas, viz., cometary comae [2], upper regions of Titan's atmosphere [3–5], plasmas in the D- and F-regions of Earth's ionosphere [4–6], and also

in laboratory environments, viz., $H^+ - O_2^-$ [8,10,13–16], (K^+, SF_6^-) plasma [7,8], $Xe^+ - SF_6^-$ [14–16,54], $H^+ - H^-$ [8,10,13–16], (Ar^+, F^-) plasma [9], plasma processing reactors [10], plasma etching [11], combustion products [11], (Xe^+, F^-) plasma [12], neutral beam sources [13], (Ar^+, SF_6^-) plasma [14–16], (Ar^+, O_2^-) plasma, Fullerene (C_{60}^+, C_{60}^-) plasma [17,18], etc.

Author Contributions: All authors contributed equally to complete this work. All authors have read and agreed to the published version of the manuscript.

Funding: The research received no external funding.

Institutional Review Board Statement: Not applicable.

Informed Consent Statement: Not applicable.

Data Availability Statement: Not applicable.

Acknowledgments: Sharmin Jahan would like to acknowledge "NST Fellowship" for their financial support to complete this work.

Conflicts of Interest: The authors declare no conflict of interest.

References

1. Shukla, P.K.; Mamun, A.A. *Introdustion to Dusty Plasma Physics*; Institute of Physics: Bristol, UK, 2002.
2. Chaizy, P.; Reme, H.; Sauvaud, J.A.; D'Uston, C.; Lin, R.P.; Larson, D.E.; Mitchell, D.L.; Anderson, K.A.; Carlson, C.W.; Korth, A.; et al. Negative ions in the coma of comet Halley. *Nature* **1991**, *349*, 393. [CrossRef]
3. Coates, A.J.; Crary, F.J.; Lewis, G.R.; Young, D.T.; Waite, J.H.; Sittler, E.C. Discovery of heavy negative ions in Titan's ionosphere. *Geophys. Res. Lett.* **2007**, *34*, L22103. [CrossRef]
4. Massey, H. *Negative Ions*, 3rd ed.; Cambridge University Press: Cambridge, UK, 1976.
5. Sabry, R.; Moslem, W.M.; Shukla, P.K. Fully nonlinear ion-acoustic solitary waves in a plasma with positive-negative ions and nonthermal electrons. *Phys. Plasmas* **2009**, *16*, 032302. [CrossRef]
6. Abdelwahed, H.G.; El-Shewy, E.K.; Zahran, M.A.; Elwakil S.A. On the rogue wave propagation in ion pair superthermal plasma. *Phys. Plasmas* **2016**, *23*, 022102. [CrossRef]
7. Song, B.; D'Angelo, N.; Merlino, R.L. Ion-acoustic waves in a plasma with negative ions. *Phys. Fluids B* **1991**, *3*, 284. [CrossRef]
8. Sato, N. Production of negative ion plasmas in a Q machine. *Plasma Sources Sci. Technol.* **1994**, *3*, 395. [CrossRef]
9. Nakamura, Y.; Tsukabayashi, I. Observation of modified Korteweg-de Vries solitons in a multicomponent plasma with negative ions. *Phys. Rev. Lett.* **1984**, *52*, 2356. [CrossRef]
10. Gottscho, R.A.; Gaebe, C.E. Negative ion kinetics in rf glow discharges. *IEEE Trans. Plasma Sci.* **1986**, *14*, 92. [CrossRef]
11. Sheehan, D.P.; Rynn, N. Negative-ion plasma sources. *Rev. Sci. Lnstrum.* **1988**, *59*, 8. [CrossRef]
12. Ichiki, R.; Yoshimura, S.; Watanabe, T.; Nakamura, Y.; Kawai, Y. Negative-ion plasma sources. *Phys. Plasmas* **2002**, *9*, 4481. [CrossRef]
13. Bacal, M.; Hamilton, G.W. H^- and D^- production in plasmas. *Phys. Rev. Lett.* **1979**, *42*, 1538. [CrossRef]
14. Wong, A.Y.; Mamas, D.L.; Arnush, D. Negative ion plasmas. *Phys. Fluids* **1975**, *18*, 1489. [CrossRef]
15. Cooney, J.L.; Gavin, M.T.; Lonngren, K.E. Soliton propagation, collision, and reflection at a sheath in a positive ion-negative ion plasma. *Phys. Fluids B* **1991**, *3*, 2758. [CrossRef]
16. Nakamura, Y.; Odagiri, T.; Tsukabayashi, I. Ion-acoustic waves in a multicomponent plasma with negative ions. *Plasma Phys. Control. Fusion* **1997**, *39*, 105. [CrossRef]
17. Oohara, W.; Hatakeyama, R. Pair-ion plasma generation using fullerenes. *Phys. Rev. Lett.* **2003**, *91*, 205005. [CrossRef]
18. Hatakeyama, R.; Oohara, W. Properties of pair-ion plasmas using fullerenes. *Phys. Scr.* **2005**, *116*, 101. [CrossRef]
19. Shukla, P.K.; Silin, V.P. Dust ion-acoustic wave. *Phys. Scr.* **1992**, *45*, 508. [CrossRef]
20. Shukla, P.K. Dust ion-acoustic shocks and holes. *Phys. Plasmas* **2000**, *7*, 1044. [CrossRef]
21. Baluku, T.K.; Hellberg, M.A.; Kourakis, I.; Saini, N.S. Dust ion acoustic solitons in a plasma with kappa-distributed electrons. *Phys. Plasmas* **2010**, *17*, 053702. [CrossRef]
22. Sultana, S.; Islam, S.; Mamun, A.A. Envelope solitons and their modulational instability in dusty plasmas with two-temperature superthermal electrons. *Astrophys. Space Sci.* **2014**, *351*, 581. [CrossRef]
23. Yasmin, S.; Asaduzzaman, M.; Mamun, A.A. Dust ion-acoustic shock waves in nonextensive dusty plasma. *Astrophys. Space Sci.* **2013**, *343*, 245. [CrossRef]
24. Rahman, A.; Kourakis, I.; Qamar, A. Electrostatic solitary waves in relativistic degenerate electron-positron-ion plasma. *IEEE Trans. Plasma Sci.* **2015**, *43*, 974. [CrossRef]
25. Abdelsalam, U.M.; Moslem, W.M.; Shukla, P.K. Ion-acoustic solitary waves in a dense pair-ion plasma containing degenerate electrons and positrons. *Phys. Lett. A* **2008**, *372*, 4057. [CrossRef]

26. Carins, R.A.; Mamun, A.A.; Bingham, R.; Dendy, R.O.; Nairn, C.M.C.; Shukla, P.K. Electrostatic solitary structures in non-thermal plasmas. *Geophys. Res. Lett.* **1995**, *22*, 2709. [CrossRef]
27. Haider, M.M.; Sultana, I.; Khatun, S.; Nasrin, J.; Tasniml, N.; Rahman, O.; Akter, S. Nonthermal distribution of electro-negative light-ions in heavy-ion-acoustic solitary and shock structures. *Theor. Phys.* **2019**, *4*, 124. [CrossRef]
28. Pakzad, H.R.; Javidan, K. Dust acoustic solitary and shock waves in strongly coupled dusty plasmas with nonthermal ions. *Pramana* **2009**, *73*, 913. [CrossRef]
29. Ghai, Y.; Saini, N.S.; Eliasson, B. Landau damping of dust acoustic solitary waves in nonthermal plasmas. *Phys. Plasmas* **2018**, *25*, 013704. [CrossRef]
30. Sabetar, A.; Dorranian, D. Effect of obliqueness and external magnetic field on the characteristics of dust acoustic solitary waves in dusty plasma with two-temperature nonthermal ions. *J. Theor. Appl. Phys.* **2015**, *9*, 150.
31. Shahmansouri, M.; Mamun, A.A. Dust-acoustic shock waves in a magnetized non-thermal dusty plasma. *J. Plasma Phys.* **2014**, *80*, 593. [CrossRef]
32. Malik, H.K.; Srivastava, R.; Kumar, S.; Singh, D. Small amplitude dust acoustic solitary wave in magnetized two ion temperature plasma. *J. Taibah Univ. Sci.* **2020**, *14*, 417. [CrossRef]
33. Islam, M.K.; Biswas, S.; Chowdhury, N.A.; Mannan, A.; Salahuddin, M.; Mamun, A.A.D. Obliquely propagating ion-acoustic shock waves in a degenerate quantum plasma. *Contrib. Plasma Phys.* **2022**, *62*, e202100073. [CrossRef]
34. Bedi, C.; Gill, T.S.; Bains, A.S. Four component magnetized dusty plasma containing non-thermal electrons. *J. Phys. Conf. Ser.* **2010**, *208*, 012037. [CrossRef]
35. Adhikary, N.C. Effect of viscosity on dust-ion acoustic shock wave in dusty plasma with negative ions. *Phys. Lett. A* **2012**, *376*, 1460. [CrossRef]
36. Sahu, B.; Sinha, A.; Roychoudhury, R. Nonlinear features of ion acoustic shock waves in dissipative magnetized dusty plasma. *Phys. Plasmas* **2014**, *21*, 103701. [CrossRef]
37. Atteya, A.; Sultana, S.; Schlickeiser, R. Dust-ion-acoustic solitary waves in magnetized plasmas with positive and negative ions: The role of electrons superthermality. *Chin. J. Phys.* **2018**, *56*, 1931. [CrossRef]
38. El-Nabulsi, R.A. Time-nonlocal kinetic equations, jerk and hyperjerk in plasmas and solar physics. *Adv. Space Phys.* **2018**, *61*, 2914. [CrossRef]
39. El-Nabulsi, R.A. Non-standard magnetohydrodynamics equations and their implications in sunspots. *Proc. R. Soc. A* **2020**, *476*. [CrossRef]
40. El-Labany, S.K.; Behery, E.E.; El-Razek, H.N.A.; Abdelrazek, L.A. Shock waves in magnetized electronegative plasma with nonextensive electrons. *Eur. Phys. J. D* **2020**, *74*, 104. [CrossRef]
41. Ourabah, K.; Gougam, L.A.; Tribeche, M. Nonthermal and suprathermal distributions as a consequence of superstatistics. *Phys. Rev. E* **2015**, *91*, 012133. [CrossRef]
42. Davis, S.; Avaria, G.; Bora, B.; Jain, J.; Morcao, J.; Pavez, C.; Soto, L. Single-particle velocity distributions of collisionless, steady-state plasmas must follow superstatistics. *Phys. Rev. E* **2019**, *100*, 023205. [CrossRef]
43. Ourabah, K. Demystifying the success of empirical distributions in space plasmas. *Phys. Rev. Res.* **2020**, *2*, 023121. [CrossRef]
44. Beck, C.; Cohen, E.G.D. Superstatistics. *Phys. A Stat. Mech. Its Appl.* **2003**, *322*, 267. [CrossRef]
45. Hussain, S.; Mahmood, S. Korteweg-de Vries Burgers equation for magnetosonic wave in plasma. *Phys. Plasmas* **2011**, *18*, 052308. [CrossRef]
46. Michael, M.; Willington, N.T.; Jayakumar, N.; Sebastian, S.; Sreekala, G.; Venugopal, C. Korteweg–deVries–Burgers (KdVB) equation in a five component cometary plasma with kappa described electrons and ions. *J. Theor. Appl. Phys.* **2016**, *10*, 289. [CrossRef]
47. Lu, D.; Seadawy, A.; Yaro, D. Analytical wave solutions for the nonlinear three-dimensional modified Korteweg-de Vries-Zakharov-Kuznetsov and two-dimensional Kadomtsev-Petviashvili-Burgers equations. *Res. Phys.* **2019**, *12*, 2164. [CrossRef]
48. Washimi, H.; Taniuti, T. Propagation of Ion-Acoustic Solitary Waves of Small Amplitude. *Phys. Rev. Lett.* **1966**, *17*, 996. [CrossRef]
49. Hossen, M.M.; Nahar, L.; Alam, M.S.; Sultana, S.; Mamun, A.A. Electrostatic shock waves in a nonthermal dusty plasma with oppositely charged dust. *High Energy Density Phys.* **2017**, *24*, 9. [CrossRef]
50. Shikha, R.K.; Orani, M.M.; Mamun, A.A. Roles of positively charged dust, ion fluid temperature, and nonthermal electrons in the formation of modified-ion-acoustic solitary and shock waves. *Results Phys.* **2021**, *27*, 104507. [CrossRef]
51. Nakamura, Y.; Bailung, H.; Shukla, P.K. Observation of Ion-Acoustic Shocks in a Dusty Plasma. *Phys. Rev. Lett.* **1999**, *83*, 1602. [CrossRef]
52. Karpman, V.I. *Nonlinear Waves in Dispersive Media*; Pergamon Press: Oxford, UK, 1975.
53. Hasegawa, A. *Plasma Instabilities and Nonlinear Effects*; Springer: Berlin, Germany, 1975.
54. Nakamura, Y.; Bailung, H.; Lonngren, K.E. Oblique collision of modified Korteweg–de Vries ion-acoustic solitons. *Phys. Plasmas* **1999** *6*, 3466. [CrossRef]
55. Oohara, W.; Date, D.; Hatakeyama, R. Electrostatic waves in a paired Fullerene-ion plasma. *Phys. Rev. Lett.* **2005**, *95*, 175003. [CrossRef] [PubMed]
56. Jahan, S.; Sharmin, B.E.; Chowdhury, N.A.; Mannan, A.; Roy, T.S.; Mamun, A.A. Electrostatic ion-acoustic shock waves in a magnetized degenerate quantum plasma. *Plasma* **2021**, *4*, 426. [CrossRef]

57. Akter, J.; Chowdhury, N.A.; Mannan, A.; Mamun, A.A. Dust-acoustic envelope solitons in an electron-depleted plasma. *Plasma Phys. Rep.* **2021**, *47*, 725. [CrossRef]
58. Islam, M.K.; Noman, A.A.; Akter, J.; Chowdhury, N.A.; Mannan, A.; Roy, T.S.; Salahuddin, M.; Mamun, A.A. Modulational instability of dust-ion-acoustic waves in pair-ion plasma having non-thermal non-extensive electrons. *Contrib. Plasma Phys.* **2021**, *61*, e202000214. [CrossRef]
59. Banik, S.; Heera, N.M.; Yeashna, T.; Hassan, M.; Shikha, R.K.; Chowdhury, N.A.; Mannan, A.; Mamun, A.A. Modulational instability of ion-acoustic waves and associated envelope solitons in a multi-component plasma. *Gases* **2021**, *1*, 148–155. [CrossRef]
60. Alinejad, H. Dust ion-acoustic solitary and shock waves in a dusty plasma with non-thermal electrons. *Astrophys. Space Sci.* **2010**, *327*, 131. [CrossRef]